Welding in the World
https://doi.org/10.1007/s40194-026-02458-3

RESEARCH PAPER

Corrosion protection and fatigue performance of HFMI-treated welded joints in offshore wind turbine structures

Daniel Löschner[1] · Imke Engelhardt[2] · Diba Kopic[3] · Stefanos Gkatzogiannis[4] · Philipp Weidner[3] · Thomas Ummenhofer[3]

Received: 6 October 2025 / Accepted: 10 April 2026

Abstract
This study investigates the fatigue performance of HFMI-treated welded joints in offshore wind turbine monopile foundations. Fatigue tests were carried out on longitudinal butt welds (LB) and T-butt welds (TB) made from S355J2 + N, S355ML, and S500ML in both as-welded (AW) and HFMI-treated conditions. In addition, single-sided transverse stiffeners (TS) were tested after blast cleaning to simulate conventional surface preparation prior to coating. The results show that HFMI significantly improves the fatigue strength of TB welds, shifting the failure location away from the critical weld toe when all weld toes, including intermediate layers, are treated. In contrast, LB welds exhibited a high fatigue resistance already in AW condition, indicating limited benefit of HFMI treatment under axial loading. Blast cleaning, whether applied before or after HFMI, was found to be compatible with organic coatings and thermal sprayed zinc and did not reduce fatigue performance; a slight positive effect was even observed. These findings support the selective use of HFMI treatment for critical details in offshore monopiles and confirm its compatibility with standard corrosion protection systems.

Keywords HFMI · Fatigue · Longitudinal butt weld · T-butt joints · Transverse stiffener · Surface preparation · Blast cleaning · Coating

Recommended for publication by Commission XIII - Fatigue of Welded Components and Structures

✉ Daniel Löschner
daniel.loeschner@unibw.de

Imke Engelhardt
imke.engelhardt@hm.edu

Diba Kopic
diba.kopic@kit.edu

Stefanos Gkatzogiannis
gkatzogiannis.stefanos@ucy.ac.cy

Philipp Weidner
philipp.weidner@kit.edu

Thomas Ummenhofer
thomas.ummenhofer@kit.edu

[1] Department of Structural Engineering, University of the Bundeswehr Munich, Neubiberg, Germany

[2] Institute for Material and Building Research, University of Applied Science Munich, Munich, Germany

[3] KIT Steel and Lightweight Structures, Karlsruhe Institute of Technology, Karlsruhe, Germany

[4] Department of Architecture, University of Cyprus, Nicosia, Cyprus

1 Introduction

The construction of offshore wind turbines (OWT) plays a key role in securing the energy supply from renewable sources. The further expansion of offshore wind energy requires a careful consideration of the dynamic boundary conditions since increasing turbine capacities and the relocation to deeper waters further increase the structural capacity demand placed on offshore support structures. Verifying the fatigue strength of welded joints remains a major challenge due to the high cyclic loading conditions. To meet these requirements, thicker steel plates are often required to reduce the local stresses. A promising measure to optimise material usage is a post-weld treatment of welded joints, particularly by high-frequency mechanical impact treatment (HFMI). Applying HFMI on high-strength steels can further enhance the benefits of this method, resulting in a reduction in total weight, lower construction and transportation costs, and reduced overall resource consumption. Compared to conventional treatment techniques such as grinding, HFMI significantly improves the fatigue strength of welded joints.

Published online: 30 April 2026

These advantages make HFMI an attractive technique for application in OWT structures.

However, there are still considerable challenges regarding the durability of corrosion protection systems on HFMI-treated weld toes. Since direct studies on coating adhesion on HFMI-treated weld toes are scarce, insight can be gained from investigations on related mechanical surface strengthening processes. Recent studies have shown that shot peening can significantly improve the adhesion of organic paint coatings on steel substrates. These improvements are mainly attributed to changes in surface topography and surface roughness, which enhance mechanical interlocking between the coating and the substrate. Experimental investigations demonstrate that peening-induced surface texture parameters strongly influence coating adhesion strength, while compressive residual stresses play a secondary role for organic systems [1–3].

It should be noted, however, that the surface modifications introduced by shot peening are not directly comparable to those generated by HFMI treatment. Shot peening typically produces a finely distributed surface roughness that is considerably lower than the roughness achieved by conventional clean blasting, which is commonly required as standard surface preparation to ensure sufficient adhesion of organic coating systems. In contrast, HFMI introduces a localised, linear geometric indentation at the weld toe rather than a two-dimensional increase in surface roughness. As a result, the HFMI-treated zone may locally promote coating accumulation due to the geometric notch, while at the same time HFMI can generate relatively smooth or shiny surface areas depending on the device and parameters used. Such surface characteristics may locally reduce coating adhesion strength if not followed by appropriate surface preparation. Therefore, while findings from shot-peening studies support the assumption that HFMI does not inherently impair coating adhesion, a direct transfer of these results is not possible. Careful validation of the combined effects of HFMI-induced geometry and subsequent surface preparation—particularly under offshore-relevant clean blasting procedures—is therefore required. The results of the present study indicate that HFMI treatment combined with conventional clean blasting does not adversely affect fatigue performance and can be successfully integrated into standard coating procedures.

In addition, no specific guidelines or systematic quality requirements currently exist to ensure the process reliability and long-term performance of HFMI-treated weld toes in combination with corrosion protection systems. The combined assessment of HFMI treatment and offshore-relevant coating systems therefore represents a critical research gap, as offshore monopile foundations rely simultaneously on mechanical fatigue resistance and long-term coating durability. The present study directly addresses this gap by linking fatigue testing of HFMI-treated details with their compatibility with conventional surface preparation (clean blasting) and subsequent coating procedures.

A particular challenge arises from the production of monopile shell sections, which are manufactured by bending flat steel plates into a cylindrical shape and welding them longitudinally. These longitudinal welds run parallel to the main axis of the structure and thus to the dominant loading direction, making them essential for the structural integrity of the monopile. Despite their importance, the fatigue behaviour of HFMI-treated longitudinal butt welds (LB) has not yet been thoroughly investigated. While the applicability of HFMI treatment in OWT structures to improve fatigue strength is generally recognised, systematic investigations are required to ensure its reliable integration into the design and manufacturing process chain over the entire service life.

This study presents the results of the research project P 1454 [4] aimed at integrating HFMI treatment into the process chain of manufacturing OWTs, thereby enabling more economical designs. The study focuses on the application of HFMI to the primary support structure of OWTs—the monopile foundation. The results show the compatibility of HFMI-treated welds with corrosion protection systems, the achievable fatigue performance under offshore-relevant loading conditions of single-sided TS, longitudinal butt joints, and T-butt joints as well as the effects on fatigue design and quality assurance.

1.1 Potential of HFMI treatment in monopile foundation structures

The monopile represents the most widely deployed foundation concept for OWTs. It comprises a single cylindrical pile upon which the turbine structure is mounted. The shell segments are manufactured from hot-rolled flat steel plates, which are cold-bent into a cylindrical or conical shape and subsequently joined along longitudinal seams. These longitudinal welds are typically applied from both the inside and outside. These sections are subsequently joined by circumferential butt welds to produce larger segments, which are then welded together along the "growing line" to assemble the complete monopile structure. Normal strength steels in accordance with DIN EN 10025-1 [5] and EN 10025-3 [6] are predominantly used for the primary support structure [7]. Monopiles are considered the most economical foundation solution for water depths of up to approximately 50 m. Hybrid construction methods that combine monopiles with floating foundation technologies have extended the feasible installation depth to around 100 m. With increasing water depths, the stresses acting on the supporting structures also rise significantly. The combination of cyclic mechanical loading with environmental influences such as temperature fluctuations, UV radiation, and corrosive seawater exposure subjects these welded structures to a severe fatigue loading.

As a result, increased wall thicknesses are often adopted in the design process to meet the fatigue strength requirements of welded joints.

However, the use of higher strength steels in conjunction with post-weld treatment techniques such as high-frequency mechanical impact (HFMI) offers a viable approach in order to reduce the resource consumption and optimise the material utilisation while maintaining or improving fatigue performance [8–11]. Recent studies have demonstrated that HFMI treatment is effective in significantly improving the fatigue strength of uncoated welded joints exposed to corrosive environments under short-term laboratory conditions [8–11]. These exposure durations overlap with typical offshore wind turbine (OWT) inspection intervals and have been correlated with real marine corrosion scenarios based on previous experimental research [8]. The initial findings suggest that applying HFMI to welded joints in offshore structures is a safe strategy for reducing material usage, as the increased fatigue strength allows for thinner plate sections or a reduced weld reinforcement. This benefit remains relevant even in cases where protective coatings may fail unexpectedly between inspection and repair intervals. Therefore, the use of HFMI in OWT applications shows considerable potential. Additionally, research work in recent years has increasingly focused on improving the efficiency and reproducibility of HFMI treatment, particularly regarding its integration into automated fabrication processes. Wendler et al. [12] investigated the use of robotic systems for HFMI treatment of welded joints. These findings demonstrate that automation can significantly enhance process accuracy and ensure consistent quality of HFMI-treated welds, thereby further increasing the efficiency and industrial applicability of HFMI.

Parallel to the advancement of automation, efforts have been made to establish quality assurance procedures for HFMI treatment. Early recommendations, originally developed for conventional hammer peening processes [13], were adapted for HFMI [14, 15]. Experimental studies have confirmed that both under- and overtreatment within defined boundaries lead to only moderate reductions in the effectiveness of HFMI [16, 17]. However, due to the variety of available HFMI devices and treatment parameters, standardisation based solely on equipment parameters is not feasible. Instead, quality assurance must rely on the visual inspection of the treated weld toe [16–18]. A smooth surface finish and an adequate indentation depth are regarded as indicators of a proper treatment [16–20]. In most recent work, the HFMI treatment's impact energy has been also applied as a quality assurance indicator [20].

Based on these developments, the International Institute of Welding (IIW) published comprehensive guidelines for the application, quality control, and fatigue design of HFMI-treated welds [21]. Improved FAT classes for nominal stress approaches are provided based on the stress ratio and the base material; the size and thickness effects for plates thicker than 25 mm are presented by Hobbacher [22]. Complementary national regulations such as the German DASt Guideline 026 [23] specify the requirements for fatigue assessment of welded joints treated with qualified HFMI methods (HiFIT, PIT, UIT). The guideline covers specific detail categories, including transverse attachments and butt welds, and outlines additional fabrication requirements to ensure the feasibility of the post-weld treatment.

One critical aspect not yet fully addressed in existing guidelines is the treatment of certain weld details beyond the scope of DASt Guideline 026 [23], such as LB and TB as shown in Fig. 6. Furthermore, the effect of a surface preparation following a post-weld treatment, such as blast cleaning after HFMI treatment, remains an open topic. According to DASt Guideline 026, blast cleaning is permitted after HFMI treatment to achieve the surface conditions required for the long-term performance of organic corrosion protection systems. Preliminary studies [24] suggest that blast cleaning may be compatible in order to maintain the improved fatigue performance of HFMI-treated welds, but further research is needed to confirm whether current fatigue design approaches for HFMI-treated welds remain valid following standard surface preparation procedures used in offshore steel construction.

1.2 Corrosion protection for offshore wind energy turbines

Offshore wind energy turbines are exposed to extreme weather conditions. These include environmental influences such as marine or industrial atmospheres, extreme temperature fluctuations, intense UV radiation, and high humidity. As a result, the highest corrosivity category CX according to DIN EN ISO 12944 [25] applies. Accordingly, suitable measures are required to ensure the durability of these structures. These measures are critical to guarantee the intended service life and efficiency of the installations. The selection of a suitable corrosion protection system is a complex task that requires a combination of various technologies and strategies as well as the consideration of numerous location factors. One such factor is the exposure location on the structure. Depending on the position relative to the waterline, wind energy installations are divided into four corrosion zones. These zones are illustrated using the example of a monopile in Fig. 1 [26]. The highest corrosive erosion occurs in the splash water zone (swz). The alternating wet-dry cycles in this area lead to high corrosion rates [27, 28]. For this reason, special attention must be paid to these areas when designing corrosion protection systems. Additionally, a distinction is made between the internal and external surfaces of

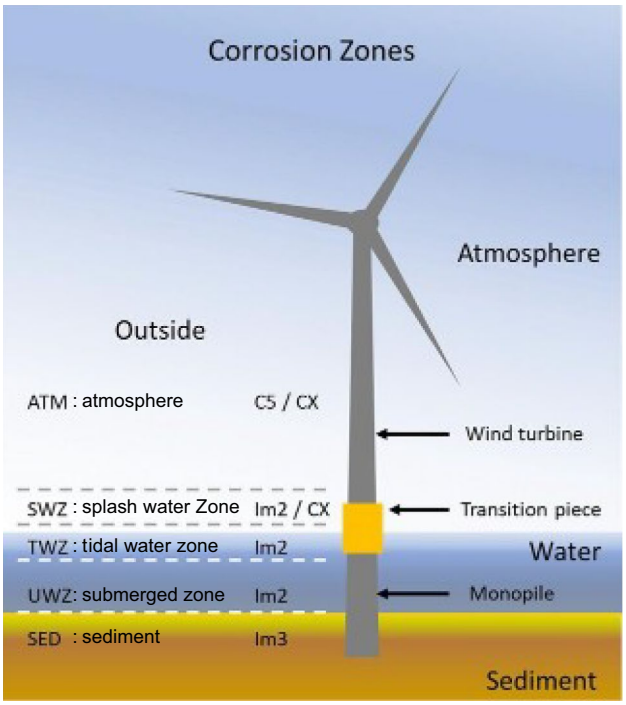

Fig. 1 Illustration of the external corrosion zones of an offshore monopile

the structure. Among the various approaches available, passive corrosion protection is the most applied method. This preference is due to its proven long-term durability, compatibility with large-scale steel structures, and the ability to be standardised and quality-controlled in both manufacturing and field conditions.

Passive corrosion protection includes strategies that prevent corrosion without the need for electrical or electrochemical interventions. The core principle lies in creating a physical barrier between the steel surface and the corrosive environment, primarily using coatings and surface treatments.

For offshore structures, organic coatings, such as epoxy or polyurethane systems, are widely used. These are typically applied in multiple layers to achieve an optimal performance:

- The primer ensures adhesion to the metallic substrate and provides the base for the entire coating system.
- An intermediate layer enhances corrosion resistance and reinforces the adhesion of the topcoat.
- The topcoat serves as the outermost protective layer, resisting weathering, UV radiation and mechanical impacts.

Another widely used passive protection technique is thermal metal spraying (metalising), particularly suited for large, exposed surfaces. In this process, molten metal—typically zinc or aluminium—is sprayed onto the prepared steel surface, forming a durable and corrosion-resistant layer.

An effective performance of passive protection systems depends heavily on proper surface preparation, which typically involves dry blast cleaning. This process removes contaminants such as rust, old coatings and grease, while also roughening the surface to ensure mechanical adhesion of the coating. Standards such as ISO 8501-1 [29] and ISO 8503-1 [30] specify the required cleanliness grade (Sa 2½) and roughness level ("medium (G)"), respectively. For offshore applications, steel grit at a pressure of 6 to 8 bar is commonly used to meet these requirements. After surface preparation, coating systems are applied and tested regarding performance and durability. Standards such as ISO 12944-4 [25], ISO 12944-5 [31], and ISO 12944-9 [32] provide guidance on the design, application, and testing of corrosion protection systems under offshore conditions. Given the extreme corrosivity of marine environments, passive corrosion protection remains the standard approach for OWTs due to its low maintenance requirements, broad in situ experience, and cost-effective implementation over the service life of these structures. Significant challenges remain regarding the long-term effectiveness of corrosion protection systems applied to HFMI-treated welds. The adhesion of organic surface coatings on these HFMI-treated zones has not yet been sufficiently investigated, leading to uncertainties concerning their long-term durability. Moreover, there are currently no specific regulations or systematic quality requirements to ensure process reliability and effectiveness of HFMI treatments throughout the service life of offshore structures.

2 Experimental work

To support the integration of HFMI treatment into industrial fabrication processes for offshore wind structures, a series of experimental investigations were carried out, focusing on selected aspects relevant to production and design. The study examined the surface characteristics of HFMI-treated weld zones with respect to their compatibility with subsequent blast cleaning and the adhesion of organic coating systems. In addition, the fatigue performance of welded and HFMI-treated TS after surface preparation by blasting was evaluated to assess the combined effect of a mechanical post-weld treatment and coating-related processing steps. Beyond this, two additional welded joint types commonly used in offshore structures, which are not yet covered by existing fatigue design recommendations and for which no HFMI-related experimental data is available, were investigated in order to assess their performance for fatigue design and for standardisation work in future.

All HFMI treatments conducted in this study followed the qualified methods HiFIT and PITEC. The specific treatment parameter variations for each specimen type, including pin diameter, operating frequencies, and application angles, are described in the corresponding subsections.

2.1 Corrosion protection of HFMI-treated welds

2.1.1 Corrosion tests in artificial atmospheres

Salt spray test The salt spray test according to DIN EN ISO 9227 [33] is a widely used method for evaluating the corrosion resistance of metallic materials, with or without permanent or temporary corrosion protection. In the neutral salt spray (NSS) test, a 5% sodium chloride solution is sprayed on the specimen in a controlled environment. The pH value and temperature inside the salt spray chamber are monitored in accordance with the specifications of DIN EN ISO 9227 [33]. The corrosion exposure duration of the test specimens in the chamber (Fig. 2) depends on the expected corrosion resistance of the material or corrosion protection system being tested. During the exposure period, the specimens are regularly inspected for indications of corrosion. After corrosion exposure, the specimens are rinsed with deionised water to remove loosely attached corrosion products. The assessment of corrosion attack can be done qualitatively visually, but it can also be quantified, measuring the reduced mass or respective dimensions. The number, the condition, and the geometry of the test specimens must be determined regarding the intended future application. Particular attention has to be paid to the positioning of the specimens in the salt spray chamber. The specimens are arranged at an upward angle of 20° from the vertical direction to ensure that they are not directly hit by the salt spray jet. To achieve this, appropriate holders—e.g. made of polypropylene material—must be fabricated, taking the respective specimen geometry into account.

Fig. 2 Salt spray chamber, located in the laboratory of the Institute for Steel, Timber, and Masonry Structures

Fabrication of small-scale specimens In total, specimens for three test series were manufactured. As presented in Table 1, series 1 and 2 differ in the sequence of manufacturing steps. In series 1, after welding a blind seam using a GMAW process, the HFMI treatment was performed by the respective HFMI device manufacturer. Therefore, appropriate intensity settings for the steel grade S355 J2 were applied. Subsequently, the corrosion test sides of the plates were blast cleaned with angular abrasive material in order to reach at least a surface preparation grade Sa 2½, as defined in ISO 8501-1 [29]. The surface profile on the corrosion test side of each plate corresponded to grade "medium (G)" according to ISO 8503-1 [30], which was verified using a comparator as described in ISO 8503-2 [34]. In series 2, the manufacturing steps were performed in a reverse order compared to series 1 after welding the blind seam. Finally, a corrosion protection system was applied according to the manufacturer's specifications. In series 3, the blind seam was ground flush after welding. The corrosion test sides were then blast cleaned to a surface preparation grade Sa 2 and the corrosion protection system was applied. Regarding the corrosion protection systems used, an organic coating system with and without a primer as well as thermal zinc spraying was investigated. Figure 3 shows small-scale specimens without and with the respective corrosion protection systems. The coating systems used are presented in Table 1. In total, a number of 24 small-scale specimens (8 specimens for each series) were manufactured. The corrosion protection systems used in the experimental programme are summarised in Table 2.

Suitability testing of the selected coating systems and surface preparations To evaluate the corrosion resistance of the selected coating systems and surface preparation methods, the small-scale specimens were exposed to a corrosive atmosphere in a salt spray chamber according to DIN EN ISO 9227 [33]. The salt spray chamber, located in the KIT Steel and Lightweight Structures laboratory and

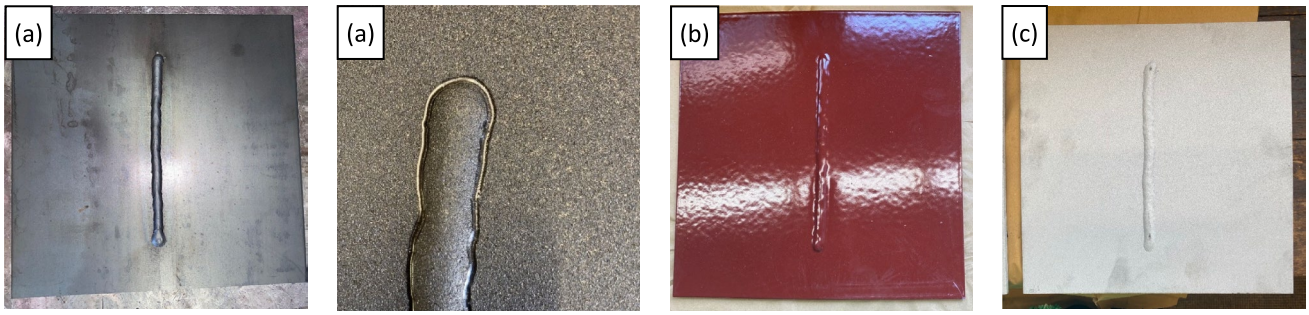

Fig. 3 Small-scale specimens (AW and HFMI-treated) without a coating (**a**), with organic coating (**b**), and thermal zinc spray (**c**)

Fig. 4 Polypropylene holder for the small-scale specimens

manufactured by Erichsen (Hemer-Sundwig), is approved exclusively for neutral salt spray (NSS) testing. The respective salt concentration required by DIN EN ISO 9227 [33] is regularly monitored. To position the corrosion test surfaces of the specimens at the specified angle to the spray mist, holders made of a polypropylene material were fabricated. This holder, including its dimensions and final shape, is shown in Fig. 4. The duration of corrosion exposure was set to 4200 h, based on the corrosivity category C5-M as defined in DIN EN ISO 12944-6 [35] and DIN EN ISO 12944-9 [32]. Visual inspections were carried out at three-week intervals during the corrosion exposure. Since no signs of corrosion have been observed at any inspection, the duration of exposure was extended. Finally, the specimens were removed from the salt spray chamber after 30 weeks, or 210 days, corresponding to 5040 h. (Tables 3, 4, 5, 6, 7, 8, 9, 10, 11, 12, and 13)

After the corrosion exposure period, all specimens were cleaned and visually inspected for indications of corrosion. Both the organic coating systems (with and without primer) and the thermally sprayed zinc coatings fulfilled the performance criteria referenced in Table 5 of DIN EN ISO 12944-9 [32]. As seen in Fig. 5, no evidence of rust formation, cracking, or coating delamination has been observed. Importantly, no significant differences in coating adhesion or durability were identified with respect to the sequence of surface preparation (blast cleaning) and HFMI post-weld treatment. These findings indicate that the application of HFMI treatment does not compromise the performance of the investigated coating systems. On the contrary, it may be considered compatible with standard corrosion protection procedures for welded joints exposed to high mechanical demands.

Because no scribes were applied, the absence of corrosion after 5040 h reflects the barrier performance of the intact coating systems. Modern offshore coating systems are known to withstand such exposure durations without degradation, and therefore, the present results do not allow conclusions regarding coating adhesion or rust creep behaviour under damaged conditions. Further work involving scribed specimens would be required to evaluate the interaction between HFMI-induced surface profiles and coating adhesion in the presence of coating defects.

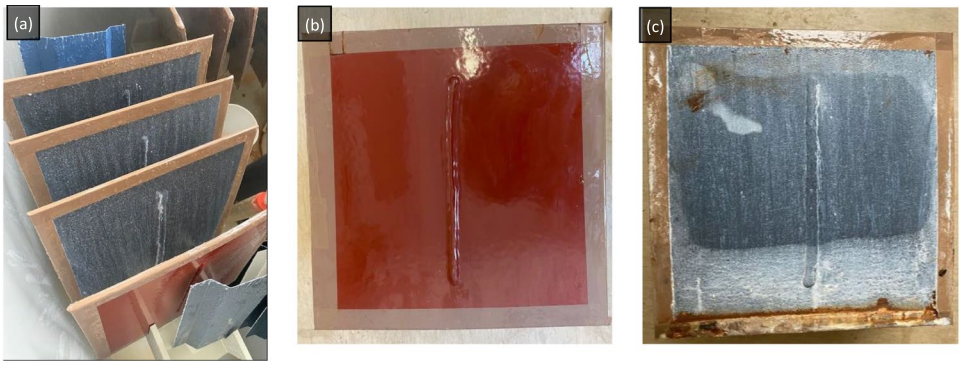

Fig. 5 Specimens in salt spray chamber after 2688 h of corrosion exposure (**a**) and after removing from the chamber after 5040 h and cleaning (**b** and **c**)

2.1.2 Surface quality requirements

The blast cleaning process effectively removes surface contaminants and increases the surface roughness, thereby enhancing the adhesion of subsequently applied coatings. The required level of surface roughness depends on the specific coating system used. Surface preparation by blasting can thus be flexibly integrated into the production process either prior to or following HFMI treatment. Considering the manufacturer-specific requirements for surface preparation and application of the selected corrosion protection systems, both adhesion and durability were confirmed in the HFMI-treated weld toe zone—regardless of the sequence of blasting and HFMI treatment. This applies to both the organic coating systems and the thermally sprayed zinc coating investigated in this study.

2.2 Specimen design for fatigue tests and weld geometry

2.2.1 Materials, fabrication, and specimen geometry

The specimens used for the fatigue tests were manufactured from normalised rolled plates of steel grade S355J2 + N according to EN 10025-2 [38] and from thermomechanical rolled plates of the steel grades S355ML and S500ML in accordance with EN 10025-4 [39]. The chemical composition and the corresponding mechanical material properties, as stated in the material test certificates 3.1 according to DIN EN 10204 [40], are summarised and outlined in Tables 3 and 4.

The welded detail longitudinal butt joint (LB) and T-butt joint (TB) were fabricated using rolled plates of the steel grades S355J2 + N, S355ML, and S500ML. The plates were cut to shape using waterjet cutting and subsequently welded using a double-V-groove weld configuration. For the T-butt joint detail, metal arc welding (GMAW) was applied, while the longitudinal butt joint was welded using submerged arc welding (SAW). For weld preparation, a groove angle of 60° and a root gap of 2 mm were applied. The final geometry of the specimens, as shown in Fig. 6, was produced by waterjet cutting as well. The cutting surfaces and edges were grinded (respectively polished and rounded) using a flap disc to mitigate potential undesired effects that could lead to early crack initiation, as such artificially cut surfaces do not occur in the vicinity of actual weldments in offshore wind turbine (OWT) structures. The single-sided TS were GMAW-welded on rolled plates of steel grades S500ML and S355J2 + N. The specimens were cut to their final geometry, as shown in Fig. 6, using a sawing process. The cutting edges were finished by grinding with a flap disc. The welding process parameters are given in Table 5.

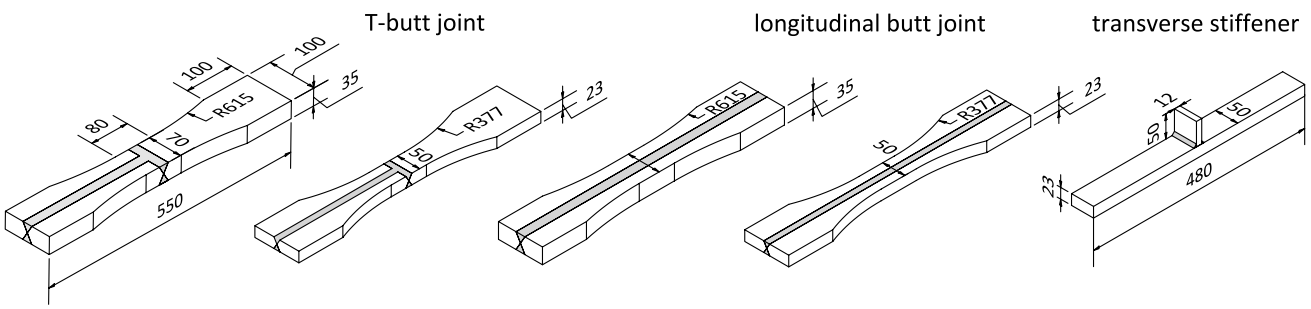

Fig. 6 Specimen geometry of T-butt joints, longitudinal butt joints, and TS

2.2.2 HFMI treatment and surface preparation

HFMI treatment was carried out using the two qualified methods HiFIT and PITEC [23]. All specimens were treated with appropriate parameters as specified by the respective equipment manufacturers. Table 6 summarises the applied treatment parameters as a function of material/steel grade, notch detail and selected treatment intensity level. For the PIT treatment, a pin diameter of 4 mm was used, whereas the HiFIT device operated with a pin diameter of 3 mm. The HFMI process produced a burr at the edge of the specimens, which was removed prior to testing by grinding.

Fatigue tests on the TS made of S355J2 + N and S500ML—after HFMI treatment followed by blast cleaning—were conducted to verify the assumption that a surface preparation, as required prior to the application of corrosion protection systems, does not adversely affect the fatigue strength of HFMI-treated components. To this end, twelve specimens of each material, previously treated with suitable HFMI parameters, were subjected to manual blast cleaning using a circular nozzle. Table 7 summarises the blasting parameters and the abrasive medium used.

Although no coating system was applied, the blasting process was carried out to meet the surface preparation requirements typically specified for corrosion protection systems. According to the requirements associated with the coating systems in the test programme (Section 2.1), a cleanliness of S_a 2½ was specified. In addition, an average surface roughness of $R_z \geq 70$ µm was required to ensure sufficient adhesion. Compliance with these parameters was verified by tactile roughness measurements in accordance with DIN EN ISO 3274 [41], with measured R_z values ranging from 72 to 141 µm.

Figure 7 illustrates the blasted surface and the weld toe area of the specimens. In some cases, grooves of the HFMI treatment remained visible after blasting. However, no correlation was found between the visibility of these marks and the HFMI method used.

2.2.3 Local weld geometry

The weld toe geometry of the TS was measured in both the AW and HFMI-treated condition using laser triangulation. A 3D profile sensor (Keyence LJV-7080) was used to capture the surface contour. The resulting point clouds were

Fig. 7 HFMI-treated specimens of the TS detail after blast cleaning

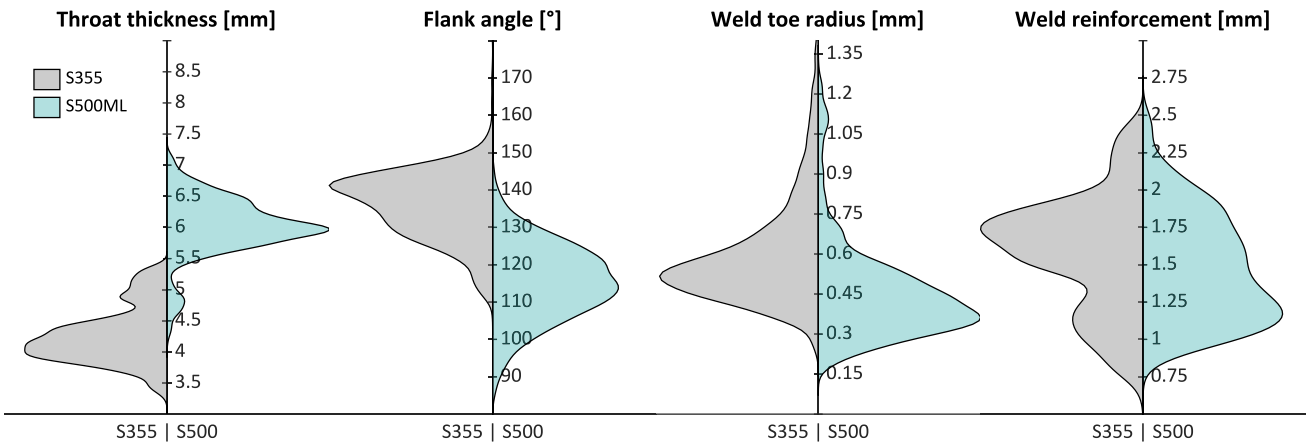

Fig. 8 Distribution of weld geometry parameters (AW) based on kernel density estimation

exported and evaluated in MATLAB using the curvature method [42]. Mean values, standard deviations, and variances of the measured geometry parameters are summarised in Table 8.

Figure 8 shows the measured weld geometry in the AW condition based on a kernel density function. For the specimens made of S500ML, the measured throat thickness exceeds the target range of 4–5 mm by approximately 1–2 mm. Compared to the specimens made of S355J2 + N, the S500ML specimens exhibit a significantly sharper weld toe transition, reflected in steeper weld flank angles. In some cases, the flank angle falls below the required value of 110° for quality level B according to ISO 5817 [43]. In contrast, the weld toe radius and the measured weld reinforcement are comparable for both material grades.

Figure 9 presents the weld toe radii and indentation depths after HFMI treatment for both materials and two different pin diameters. The HFMI-induced weld toe geometries show largely comparable characteristics for both steel grades S355J2 + N and S500ML under the applied treatment parameters. Slightly smaller radii are observed for S500 when treated with the larger pin diameter ($R_P = 2.0$ mm) compared to S355. When using the smaller pin diameter ($R_P = 1.5$ mm), TS made of S500 show a tendency towards slightly deeper indentations than specimens made of S355.

Following blast cleaning, no significant changes in HFMI-induced weld toe geometry were observed. While the HFMI groove was no longer clearly visible due to the loss of surface gloss, the measured geometry at the weld toe remained unaffected, or changes were not detectable respectively. The resulting HFMI-induced indentation geometries are summarised in Table 9.

Although the S500ML specimens exhibit a sharper weld toe flank angle than S355J2 + N specimens, this difference is not expected to significantly affect the geometric notch severity for the present detail. Previous numerical studies

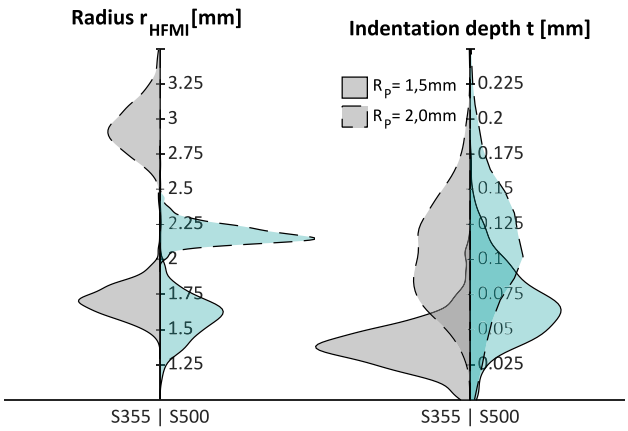

Fig. 9 Distribution of indentation depth and weld toe radius after HFMI treatment, based on kernel density estimation

[44] have shown that flank angle effects are most pronounced only at very shallow weld toe transitions ($\theta \approx 30°$), whereas steeper transitions do not lead to a meaningful increase in the stress concentration. This is consistent with our observations, as the fatigue performance of the S500ML specimens remained high despite the lower flank angle.

The notch stress level at welded joints is primarily governed by local weld geometry parameters [45]. High local stress concentrations typically occur when steep flank angles coincide with very small weld toe radii. A literature review by Baumgartner [46] confirms that welded joints such as longitudinal and transverse stiffeners or cruciform joints generally show a high geometric notch severity dominated by the weld toe radius. Accordingly, the influence of the flank angle becomes most pronounced only when the weld toe radius is very small and is of minor relevance once a sufficiently large radius is present.

HFMI treatment further modifies the local geometry by introducing a rounded weld toe profile. Studies by [43] have shown that, once the HFMI indentation depth is sufficient to fully reach and reshape the weld toe region, the resulting geometric notch effect becomes largely independent of the original flank angle. Although these investigations were performed on butt welds, the underlying mechanism is transferable. In the present study, the HFMI-treated weld toes exhibited radii of approximately $r \approx 1.5$ mm and indentation depths in the range of 0.04–0.20 mm—values consistent with the threshold at which the toe geometry becomes governed by the HFMI imprint rather than the as-welded flank angle.

This combination of a comparatively large weld toe radius and sufficient HFMI indentation provides a plausible explanation for the high fatigue strength of the S500ML specimens, despite their sharper flank angle in the as-welded condition. Under such geometric conditions, the contribution of the flank angle to the resulting notch stress is expected to be minimal.

2.3 Fatigue strength of HFMI-treated and clean-blasted transverse stiffeners

To evaluate the influence of HFMI treatment in combination with blast cleaning on fatigue performance, systematic fatigue tests were conducted on TS. The testing programme aimed to verify whether the beneficial effects of HFMI on fatigue life are maintained despite the subsequent mechanical surface treatment. All specimens were treated using specific HFMI parameters and then blasted under surface conditions representative of typical coating preparation in offshore construction. The results provide valuable insights into the interaction between post-weld treatment and surface conditioning in terms of an increase in fatigue strength.

2.3.1 Fatigue test procedure and interpretation of failure modes

Fatigue tests were performed using a high-frequency resonance pulsator with a maximum load capacity of $F_{o,max} = 600$ kN at a test frequency of 60 Hz. Additional tests were carried out on a servo-hydraulic testing machine with a maximum load of $F_{o,max} = 1000$ kN at a frequency of 7 Hz. The fatigue load was applied hydraulically via wedge grip clamping mechanisms at a stress ratio of $R = 0.1$. The areas of the specimens to be clamped were cleaned by blast cleaning to ensure a consistent load transfer. During testing, a frequency deviation of $\Delta f = \pm 0.15$ Hz and a stiffness reduction of 20% were defined as termination criteria, as empirical indicators of an initiated fatigue crack. The run-out limit for the fatigue tests was set to 5×10^6 load cycles. The test rigs are shown in Fig. 10. Fatigue tests were terminated once the defined criteria were reached, or a visible crack appeared.

Fig. 10 Servo-hydraulic test rig (left) and resonance test rig (right)

Typical failure modes of the HFMI-treated TS observed at the end of testing are shown in Fig. 11.

Several specimens exhibited cracks in the base material near the clamping area. The failures observed in the clamping region were purely mechanical in nature; no indications of fretting corrosion, surface damage, or discoloration typical of fretting processes were detected. The clamping force had been verified prior to testing and was sufficient to prevent slip between the specimen and the grips. The failures are therefore attributed to local stress concentrations at the rounded specimen edges within the grip region rather than to insufficient clamping or fretting-related mechanisms.

It was initially decided to shorten the affected specimens and to continue the tests. However, the first shortened specimen failed at the weld toe after only a few cycles, rendering this procedure impractical. Consequently, no further specimens were retested in this manner. For consistency and to avoid bias, the failures occurring in the clamping area were conservatively treated as equivalent to weld-toe failures and included in the statistical evaluation. Although these failures generally occurred at slightly higher numbers of cycles than weld-toe failures, they did not influence the statistical analysis, as they fell within the scatter band of the weld toe data.

2.3.2 Test results and statistical evaluation

The statistical evaluation of the fatigue test results was carried out according to the procedure described in [47] and [48]. Based on a regression analysis of the test data, mean S–N curves were determined for each series at a survival probability of Ps = 50%, along with the corresponding mean fatigue strength at $N = 2 \times 10^6$ cycles. The characteristic fatigue strength for a survival probability of Ps = 95% was subsequently derived using a single-sided prediction bound.

Fig. 11 HFMI-treated TS with a fatigue crack at the weld toe (top) and with a fatigue crack at the grip area (bottom)

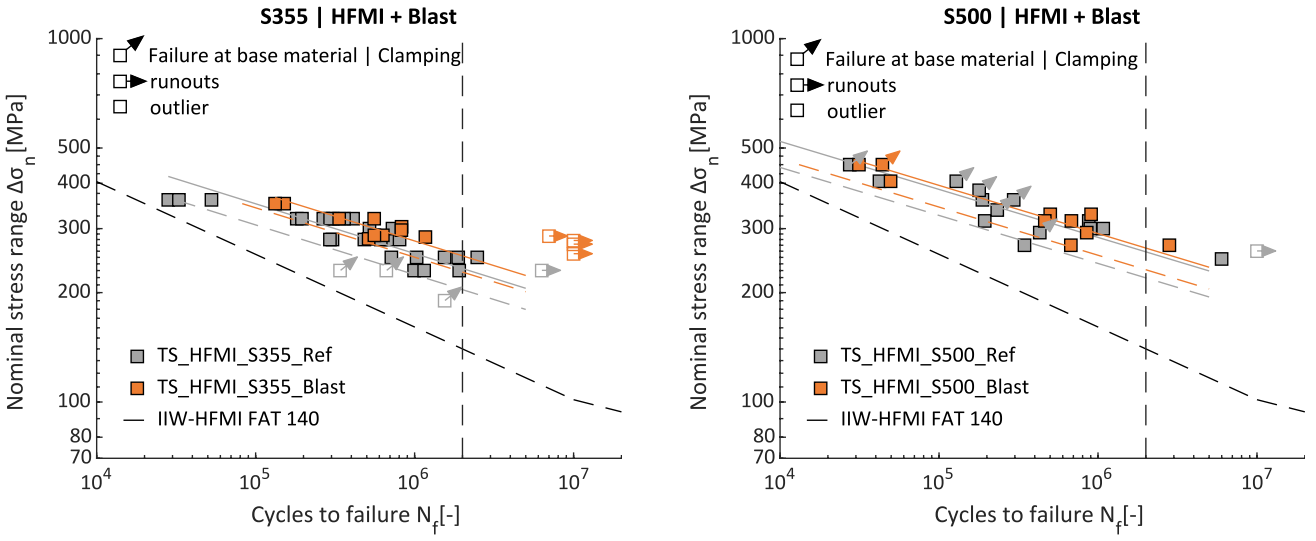

Fig. 12 Fatigue test results of HFMI-treated TS made of S355 (left) and S500 (right), with and without blast cleaning

Specimens classified as runouts or outliers were excluded from the statistical evaluation.

The results of the statistical evaluation for the specimens made of steel grade S355 without blast cleaning are presented in Fig. 12 in an S–N diagram. These specimens, which serve as a reference in the present study, are based on fatigue tests previously conducted by Wendler et al. [12]. According to the IIW recommendations [21], a fatigue strength of $\Delta\sigma_C = 140$ MPa is specified for HFMI-treated, non-load-carrying TS made of S355 at a stress ratio of $R = 0.1$. A corresponding reference S–N curve is included in the diagram for comparison. Subsequently, the results obtained from specimens subjected to additional blast cleaning after HFMI treatment are compared with these reference values to evaluate the influence of surface preparation on fatigue performance. The corresponding reference datasets for S355 and S500, used for all subsequent comparisons, are listed in Table 10.

The actual slope of the test series with blasted specimens (Q_HFMI_S355_Blast) is determined to be $m = 7.3$, which is identical to the slope of the reference series (Q_HFMI_S355_Ref.) The characteristic fatigue strength reaches 222 MPa, which is significantly higher than that of the reference series and the FAT class specified in [21]. Compared to the reference series, the scatter is reduced, with a ratio of $T_N = 1{:}2.7$. During testing, no failure was observed for specimens subjected to a stress range of $\Delta\sigma_n < 280$ MPa. These specimens were subsequently tested again at higher stress levels until a failure occurred. Following this, the prior loading history is not considered in the statistical evaluation, as a conservative approach.

As no fatigue test data for single-sided TS made of S500ML are available in the literature, a dedicated reference series (TS_HFMI_S500) was tested and analysed. The actual inverse slope of the data is determined to be $m = 7.6$, which is shallower than the slope defined by IIW [21] ($m = 5$). The mean fatigue strength for this series is calculated to 258.9 MPa, with a corresponding characteristic value of 217.2 MPa—well above the FAT class limit. The blasted specimens are evaluated in direct comparison with this reference series. The corresponding results are illustrated in detail in Fig. 12 and highlight the influence of a surface preparation following HFMI treatment on the fatigue performance. The S–N curve of the blasted S500ML specimens runs nearly parallel to the reference series, with an actual slope of $m = 7.5$. The mean fatigue strength is $\Delta\sigma_{50\%} = 265.2$ MPa, slightly exceeding that of the reference series. The characteristic fatigue strength is $\Delta\sigma_C = 228.8$ MPa, and the scatter ratio is $T_N = 1{:}3.8$, which is notably lower than that of the reference series ($T_N = 1{:}5.6$). The results of the statistical evaluation for all tested series are summarised in Table 11.

2.4 Fatigue strength of longitudinal butt welds

The test series includes the welded joint type of LB (see Fig. 6), which is representative of typical applications in offshore wind energy structures. The investigated steel grades S355J2 + N and S500ML were selected in accordance with DIN EN 10225-1 [49]. Fatigue tests were carried out in both the AW and the HFMI-treated conditions. The AW specimens serve as a reference, enabling an evaluation of the effectiveness of HFMI treatment for each series and

allowing the specific improvement to be quantified. The HFMI treatment was performed using the HiFIT device. All tests were conducted under pulsating tensile loading at a stress ratio of $R = 0.1$. The nomenclature of the test series is defined based on the plate thickness and the condition of the weld toe (AW or HFMI-treated).

2.4.1 Fatigue test procedure and interpretation of failure modes

The LB with a plate thickness of $t = 25$ mm were tested on the resonance testing rig at a frequency of 32 Hz. Fatigue tests were terminated once a displacement increase of 0.5 mm was reached. The LB with a plate thickness of $t = 35$ mm were tested using a 1 MN servo-hydraulic testing machine at a frequency between 1 and 3 Hz, depending on the applied load level. In this series, testing was stopped when a stiffness reduction of 10% was detected. The experimental setups used for fatigue testing are illustrated in Fig. 13.

In the AW series using the steel grade S355J2 + N and a plate thickness of 25 mm (LB_AW_S355_25), fatigue cracks initiated either at the rounded cut edge of the specimen or in the base material near the clamping area. Under the applied loading conditions, the longitudinal butt welds can therefore be considered non-critical with regard to fatigue performance. Although no detailed weld toe geometry measurements were carried out for the LB specimens, the failure behaviour clearly indicates that the weld toe was not the fatigue-critical location in the AW condition. The observed failure locations suggest that the AW weld geometry produced by the SAW process did not exhibit a pronounced notch effect under axial loading.

In the HFMI-treated series with S355 J2 + N and a plate thickness of 25 mm (LB_HFMI_S355_25), failures typically occurred in the form of cracks initiating at the weld cap. This was confirmed by macrosections of the

Fig. 13 Experimental setups used for fatigue testing of LB with different plate thicknesses (25 mm and 35 mm)

Fig. 14 Failure locations of LB specimens in AW and HFMI-treated conditions (S35J2 + N 5, S500ML; $t = 25/35$ mm) showing cracks at weld cap, base material, and clamping area

specimens, as illustrated in Fig. 14a–c. One specimen was excluded from the evaluation due to the presence of an internal inclusion (e). For the HFMI-treated series of the steel grade S355J2 + N and a plate thickness of 35 mm (LB_HFMI_S355_35), failures predominantly occurred in the base material or the clamping area (d). Only one specimen exhibited a crack at the weld toe.

Since HFMI primarily improves fatigue performance by mitigating geometric notch effects and introducing beneficial compressive residual stresses, its effectiveness is inherently limited when the weld toe is not the governing fatigue hotspot. This explains why the HFMI-treated and as-welded LB specimens exhibited comparable fatigue performance. The observed behaviour therefore reflects the inherently favourable AW geometry of the SAW butt welds under the given loading configuration, rather than a lack of effectiveness of HFMI for LB details in general.

Test results and statistical evaluation Figure 15 presents the results of the fatigue tests on LB for various steel grades and plate thicknesses. The diagram on the left shows the S–N curves of the results for S355 with a plate thickness of 25 mm in both the AW and HFMI-treated conditions. The right diagram includes results for HFMI-treated specimens made of S355 with $t = 35$ mm and S500ML with $t = 23$ mm. The statistical evaluation of the fatigue test results for the LB, including slopes, mean values, and characteristic fatigue strengths, is summarised in Table 12.

The statistical evaluation shows that the characteristic fatigue strengths $\Delta\sigma_{C,95\%}$ of all HFMI-treated series exceed the fatigue strength class FAT 160 defined for the base material in IIW-Recommendations [22], even when a thickness correction is applied for specimens with a thickness $t > 25$ mm. For the reference series LB_AW_S355_25, the characteristic fatigue strength is $\Delta\sigma_{C,95\%} = 245.6$ MPa based on a free slope of $m = 5{,}9$. For the HFMI-treated series with the same plate thickness, the characteristic value is $\Delta\sigma_{C,95\%} = 242.1$ MPa with a slope of $m = 6.5$.

For the HFMI-treated series with an increased plate thickness of $t = 35$ mm (LB_HFMI_S355_35), the characteristic value is $\Delta\sigma_{C,95\%} = 202.7$ MPa, based on a slope of $m = 3.6$. According to [22], the influence of plate thickness on fatigue strength must be considered (see Eq. (1)). The assignment of FAT class 160 with a slope of $m = 5$ according to the IIW Recommendations (Quelle) remains on the safe side, even when the thickness correction is applied.

$$f(t) = \left(\frac{t_{ref}}{t_{eff}}\right)^{n} \tag{1}$$

Due to the limited number of data points in the S500ML series, no statistical evaluation was performed. However, the test results indicate that failure occurred only at comparatively high stress amplitudes. The corresponding nominal stress ranges were 344 MPa (failure at the clamping area), 376 MPa and 432 MPa (failure at the weld cap). Overall, the longitudinal butt weld detail exhibits fatigue strengths that exceed both the FAT classes for base material defined in the IIW Recommendations [22] and the highest improved detail class FAT 180 specified for HFMI-treated welds in the IIW guideline on HFMI treatment [21]. For the tested configurations, HFMI treatment did not provide a significant additional benefit. Consequently, HFMI treatment of LB under uniaxial loading may be omitted, unless the detail

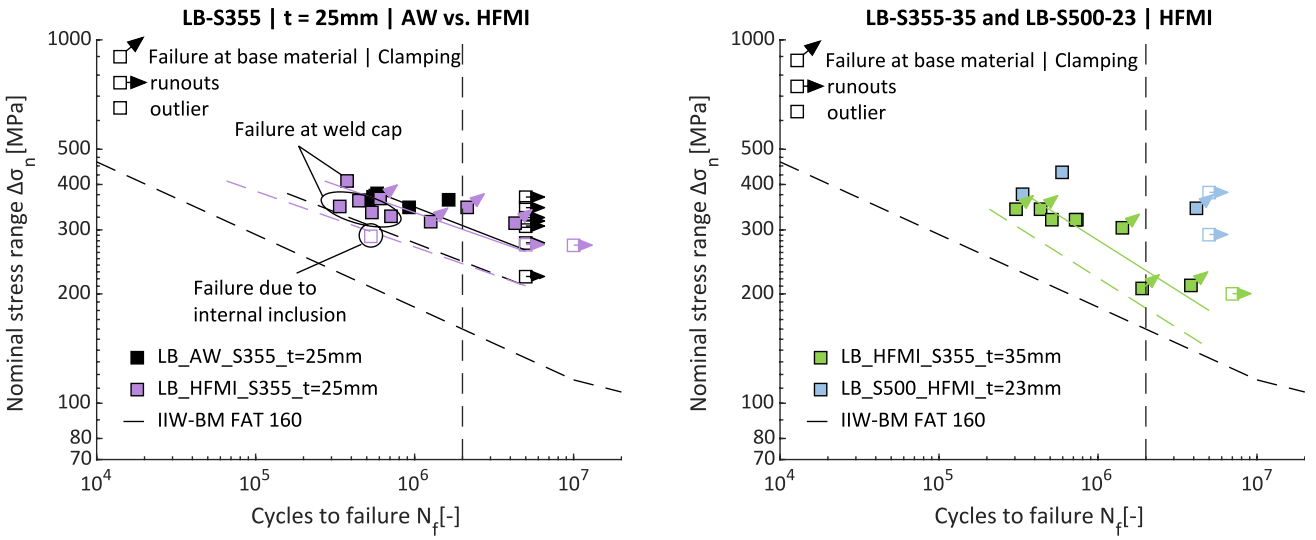

Fig. 15 Fatigue test results of longitudinal butt joints in HFMI-treated and AW conditions made of S355 (left) and S500 (right)

is part of a complex joint region (e.g. T-joints) or subjected to multiaxial loading conditions.

Fatigue strength of T-butt welds Fatigue testing of the TB specimens was carried out under the same loading conditions and evaluation criteria as applied to the LB. All tests were performed at a stress ratio of $R = 0.1$. Both AW and HFMI-treated specimens were tested to assess the effectiveness of mechanical post-weld treatment for improving the fatigue strength of this geometrically more complex detail. Fatigue tests on TB were conducted under axial tensile loading using multiple test setups, depending on plate thickness and required load levels. Specimens with a plate thickness of $t = 23$ mm were tested at frequencies of 110 Hz and 32 Hz on a high-frequency pulsator and resonance testing machine, respectively. A displacement increase of 0.5 mm was defined as the failure criterion. For the thicker specimens ($t = 34$ mm), three tests were initially performed at a frequency of 1 Hz with a displacement-based stop criterion of 0.1 mm. Due to the high loads required, the remaining specimens were tested on a servo-hydraulic testing rig at frequencies between 1 and 3 Hz, with a failure criterion defined to a 10% reduction in specimen stiffness.

Based on the failure modes shown in Fig. 16, it can be concluded that without HFMI treatment (series TS_AW_S500_23), the transverse butt weld becomes the critical location and not the longitudinal butt weld. Except for two failures observed in the intermediate layer, all cracks initiated at the weld toe of the butt weld. In the HFMI-treated series with both—HFMI-treated longitudinal and butt welds—but untreated intermediate layer (TS_HFMI_S500_23) failure predominantly occurred in the untreated intermediate layer. This failure mode changed in the series where the intermediate layer was also HFMI-treated (TS_HFMI_S500_34). A variety of failure modes was observed. Figure 16 shows representative examples, including cracks at the weld toe of the butt weld, in the intermediate layer of the transverse weld, and at the weld cap of the longitudinal weld.

In the partially treated configuration (TS_HFMI_S500_23), only the outer weld toes at the transition to the base material of the transverse and longitudinal welds were subjected to HFMI treatment, while the intermediate weld layer remained in the AW condition. Because the untreated intermediate layer retains its original weld toe geometry and residual stress state, this area represents a potential fatigue-critical zone. Furthermore, the longitudinal weld causes an additional stress concentration in this region.

Although no direct measurements of the residual stress state or hardness were conducted in this study, the fatigue lifetimes of the partially treated specimens provide sufficient support for this interpretation. In particular, one specimen exhibited a lifetime within the scatter band of the as-welded series (see Fig. 17.). This indicates that the untreated intermediate layer behaves similarly to an as-welded weld toe, which is consistent with the absence of HFMI-induced geometric modification and compressive residual stresses.

In contrast, when all accessible weld toes, including the intermediate layer, were treated (TS_HFMI_S500_34), crack initiation no longer concentrated in a single critical region but shifted between the weld toe, the weld cap, and the base material. This redistribution of failure locations is consistent with the expectation that HFMI reduces notch severity and introduces beneficial compressive residual stresses in all treated zones, thereby eliminating the dominant weak point present in the partially treated configuration.

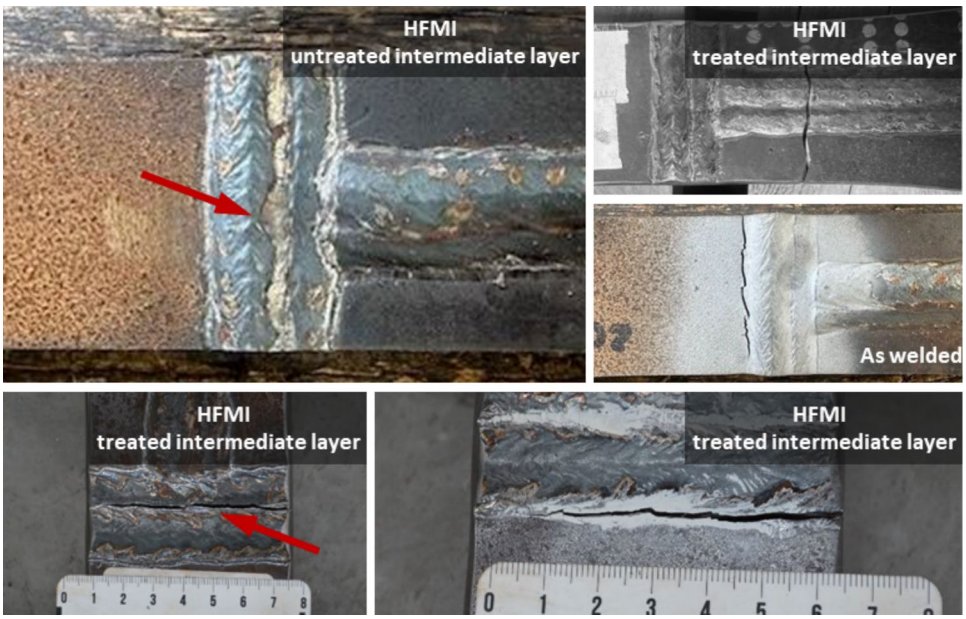

Fig. 16 Failure modes of T-butt joints in AW condition, partial HFMI treatment (without intermediate layer), and full HFMI treatment (including intermediate layer)

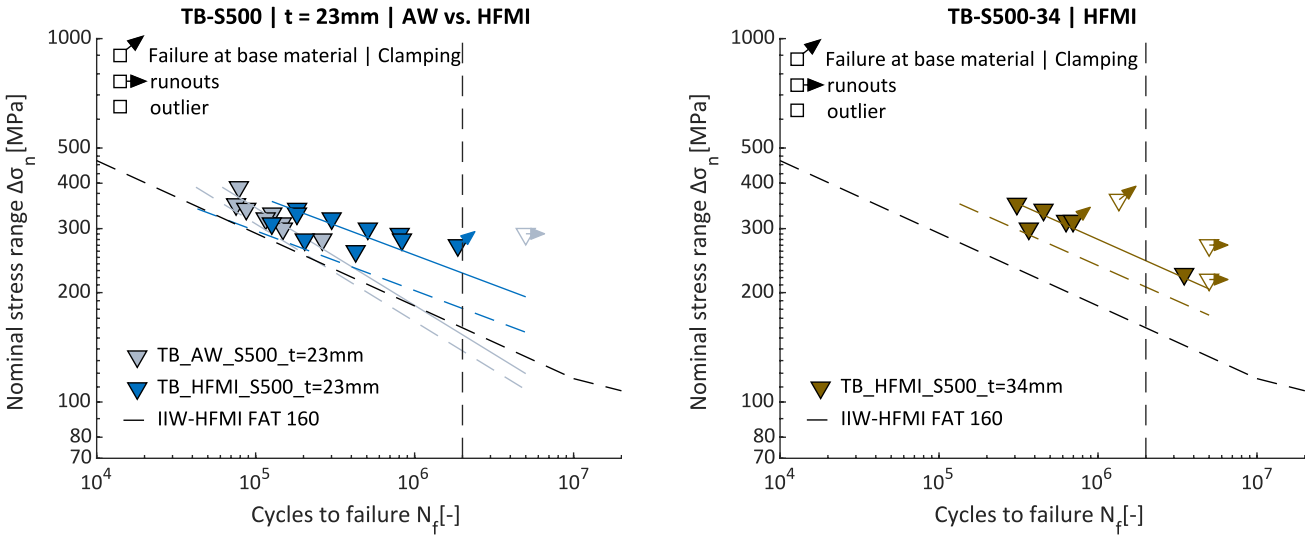

Fig. 17 Fatigue test results of transverse butt joints in HFMI-treated and AW conditions made of S500 with $t = 23$ mm (left) and $t = 34$ mm (right)

It should be noted that the term "intermediate layer" in this context refers exclusively to the outer weld passes (i.e. the surface layers) on the accessible side of the joint. These represent separate weld toes at the surface which were left untreated in the partially treated configuration. The finding does not imply that internal weld beads or root layers must be treated, nor does it require inter-pass HFMI treatment during fabrication. Only those surface-accessible weld toe transitions in the area of the adjacent longitudinal weld that remain after completion of the multi-pass weld influence the fatigue behaviour as observed in this study.

The results of the fatigue tests on T-butt joints under axial tensile loading and evaluated using a free slope are presented in Fig. 17. For the reference series TB_AW_S500_23, the characteristic fatigue strength confirms the conservativeness of the assigned fatigue class FAT 90 [22]. When evaluated with a free slope of $m = 3.7$, the characteristic value is $\Delta\sigma_{C,95\%} = 138.2$ MPa.

The HFMI-treated series TB_HFMI_S500_23 shows a significantly higher fatigue strength. With a free slope of $m = 6.0$, the characteristic value reaches $\Delta\sigma_{C,95\%} = 180.5$ MPa. The characteristic value exceeds the reference fatigue strength FAT 160 for HFMI-treated butt welds of the IIW-Recommendations [21], which assumes a comparable slope of $m = 5$. While this indicates a substantial improvement, the limited number of specimens suggests that further validation is necessary before generalisation.

In the case of the HFMI-treated series with an increased plate thickness of $t = 34$ mm (TS_HFMI_S355_34), the characteristic fatigue strength is $\Delta\sigma_{C,95\%} = 207.3$ MPa with a free slope of $m = 5.1$. Considering the thickness correction for plates with $t > 25$ mm as previously described (Eq. (1)), the adjusted characteristic value is $\Delta\sigma_{C,95\%} = 193.8$ MPa. This still exceeds the FAT 160 defined in [21] for transverse-loaded, HFMI-treated butt welds. An overview of the corresponding results is given in Table 13.

2.5 Recommendations for design practice

The findings presented in this research project [4] provide a basis for evaluating the practical relevance of HFMI treatment in the design of welded joints for offshore steel structures. While the experimental results confirm the potential for increasing the fatigue strength by HFMI treatment, they also indicate that, for some details, the expected benefit may be limited under the investigated loading conditions. In addition, the compatibility of HFMI-treated welds with standard blast cleaning procedures was confirmed, if surface quality requirements for subsequent corrosion protection are met. Overall, the research results support a differentiated approach to the use of HFMI treatment and surface preparation in offshore design practice. These recommendations are consistent with the principles outlined in the IIW-Recommendations [21] and DASt-Guideline 026 [23], while extending them to offshore-specific details such as T-butt joints and their associated corrosion protection requirements.

- LB: Under axial tensile loading, LB demonstrated a fatigue strength that exceeds both the FAT classes defined for the base material and those currently assigned to HFMI-treated welds. No significant benefit was observed from HFMI treatment. For typical applications in off-

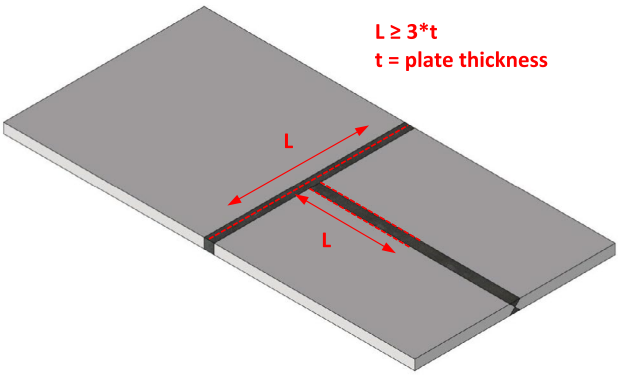

Fig. 18 Recommended HFMI treatment zones for the T-butt joint: intermediate transverse weld layer and adjacent longitudinal weld

Table 3 Mechanical material properties of steel grades S355J2C + N, S355ML, and S500ML; EN ISO 6892-1 [36] and EN ISO 148-1 [37]

Material	Thickness t (mm)	Yield strength f_y(MPa)	Ultimate strength f_u(MPa)	Elongation at fracture A (%)
S355J2 + N	20,0	424	559	28,6
S355J2 + N	25,0	431	543	35,0
S355ML	25,0	472	538	31,0
S355ML	35,0	427	523	30,0
S500ML	23,0	579	650	22,0
S500ML	34,0	596	695	23,0

shore monopile structures, HFMI treatment of LB can therefore be omitted—except in areas where the detail merges into a T-joint or is subjected to complex loading conditions.

- TB: The HFMI treatment of TB resulted in a notable improvement in fatigue strength. However, the effectiveness of the treatment strongly depends on whether the intermediate layer of the transverse weld is also included. For full benefit, HFMI treatment should be applied not only to the weld toes of the butt weld, but also to the intermediate and longitudinal weld layers within the T-joint region. A full HFMI treatment including the intermediate layer of the transverse butt weld and the adjacent longitudinal weld is therefore recommended for T-butt joints, as shown in Fig. 18. The recommendation to include the intermediate layer applies only to surface-accessible weld toe regions of the multi-pass T-joint in the area of the adjacent longitudinal weld. No interpass treatment or interruption of the welding sequence is required; HFMI can be carried out after completion of all external weld passes, provided that the geometry allows access to the respective weld toes. Consequently, no significant time or cost implications are expected for monopile production.
- Surface preparation (blast cleaning): Blast cleaning after HFMI treatment did not adversely affect the weld toe geometry or fatigue performance but even slightly increases the mean fatigue strength and reduces the scatter. Surface roughness and cleanliness levels required for coating adhesion can be achieved without compromising the beneficial effects of HFMI treatment, if blasting is conducted under controlled conditions. The surface preparation can be applied either before or after HFMI

Table 1 Fabrication steps of small-scale specimens

Small-scale specimens, steel grade S355 J2; plate thickness $t = 5$ mm, dimensions 300 × 300 mm		
Series 1	Series 2	Series 3
1 Welding the blind seam (Welding quality level B, ISO 5817)	1 Welding the blind seam (Welding quality level B, ISO 5817)	1 Welding the blind seam (Welding quality level B, ISO 5817)
2 HFMI- Treatment	2 Surface preparation Sa 2½	2 flush grinding of the weld
3 Surface preparation Sa 2½	3 HFMI-Treatment	3 Surface preparation Sa 2½
4 Application of corrosion protection coating (Coating thickness measurements according to ISO 2808)	4 Application of corrosion protection coating (Coating thickness measurements according to ISO 2808)	4 Application of corrosion protection coating (Coating thickness measurements according to ISO 2808)

Table 2 Corrosion protection systems used for preparation of small-scale specimens

Corrosion protection system	Product	Coating thickness	Manufacturer
Organic coating without primer	SikaCor® SW-501	500 µm	SIKA
Organic coating with primer	SikaCor® Zinc R, SikaCor® SW-501	60 µm, 500 µm	SIKA
Thermal zinc spray	ZnAl15	200 µm	GRILLO

Table 4 Chemical composition of plates, steel grades S355J2 + N, S355ML, and S500ML

Material	C	Mn	Si	P	S	Cr	Ni	Mo	Cu	Al	N	V	Nb	Ti
S355J2 + N (t = 20 mm)	0.16	1.41	0.23	0.015	0.004	0.086	0.069	0.015	0.178	0.035	0.007	0.004	0.011	0.002
S355J2 + N (t = 25 mm)	0.15	1.59	0.23	0.018	0.004	0.036	0.026	0.011	0.025	0.030	0.002	0.002	0.018	0.002
S355ML (t = 25 mm)	0.079	1.54	0.383	0.013	0.007	0.048	0.056	0.025	0.026	0.020	0.0053	0.001	0.020	0.002
S355ML (t = 35 mm)	0.080	1.54	0.368	0.013	0.001	0.037	0.21	0.004	0.019	0.010	0.006	0.001	0.021	0.001
S500ML (t = 23 mm)	0.083	1.678	0.425	0.017	0.0008	0.221	0.309	0.048	0.263	0.027	0.0054	0.002	0.022	0.002
S500ML (t = 34 mm)	0.086	1.695	0.469	0.016	0.0007	0.227	0.377	0.056	0.272	0.030	0.0068	0.001	0.022	0.003

Table 5 Welding process parameters for TB-, LB-, and TS-specimens of steel grades S355J2 + N, S355ML, and S500ML

Material (detail)(-)	Process (-)	Filler material (-)	Diameter (mm)	Current (A)	Voltage (V)	Polarity (-)	Wire feed (m/min)	Travel speed (cm/min)	Heat input (KJ/cm)
S355J2 + N (TS)	135	G505MG4Si1	1.2	290–310	29–31	DC +	10–1	40–45	9–11.5
S500ML (TS)	135	G505MM213Ni	1.2	280–285	30–31	DC +	10–11	35–45	11.7
S355ML (LB)	121	Böhler Union S 3 Si	4.0	580–780	26–33	DC +/AC ~	N/A	60–80	19.4–38.6
S500ML (LB)	121	Böhler Union S 3 Si	4.0	580–780	26–33	DC +/AC ~	N/A	60–80	19.4–38.6

Table 6 HFMI treatment parameters

Detail (-)	Material (-)	Intensity (-)	Frequency (Hz)	Pressure (bar)	Intensity level (°)	Speed (mm/s)	No. of passes (-)
LB/TB	S355J2 + N/S500ML	As recommended[1]	Approx. 250	6	360	10	1
TS	S355J2 + N/S500ML	As recommended[1]	Approx. 250	6	360	10	1
TS	S355J2 + N	As recommended[2]	90	5	-	6	3

[1] HiFIT device, manufacturer-recommended settings | [2] PITEC device, manufacturer-recommended settings | application angle 70° and 90° in welding direction

Table 7 Blast cleaning—abrasive medium and blasting parameters

Abrasive medium	Manufacturer	Shape	Grain size	Hardness	Distance	Angle	Pressure	Abrasive flow rate	Almen intensity
Steel grit	AMASTEEL GRIT	hard angular	G40	≥ 700 HV	1 m	45°	7.5 kg/cm^2	0.8 kg/s	L ≥ 320 µm

Table 8 Mean value, standard deviation, and coefficient of variation of the measured weld toe geometry parameters (AW)

Material	Throat thickness (mm)			Flank angle (°)			Weld toe radius AW (mm)			Weld reinforcement (mm)		
	µ σ	max min	v (%)	µ σ	max min	v (%)	µ σ	max min	v (%)	µ σ	max min	v (%)
S355J2 + N	4.20 0.44	5.37 3.26	10.42	135.81 8.95	191.77 107.18	6.59	0.60 0.20	1.60 0.23	33.16	1.61 0.42	3.11 0.62	26.10
S500ML	6.00 0.48	7.20 4.17	8.01	115.28 10.04	159.30 84.60	8.71	0.47 0.19	1.30 0.16	40.86	1.60 0.53	3.50 0.78	33.31

Table 9 Mean value, standard deviation, and coefficient of variation of the measured indentation geometries of the HFMI treatment

Material (-)	Applied pin radius R_p (mm)	Radius r_{HFMI} (mm)			Indentation depth t (mm)		
		μ σ	max min	v (%)	μ σ	max min	v (%)
S355J2 + N	1.5	1.71 0.11	2.71 1.40	6.7	0.04 0.01	0.11 0.00	44.2
	2.0	2.94 0.20	3.69 2.05	6.5	0.11 0.04	0.28 0.01	36.1
S500ML	1.5	1.59 0.17	1.95 1.14	10.7	0.07 0.03	0.17 0.00	41.2
	2.0	2.26 0.22	2.98 2.00	9.6	0.11 0.07	0.26 0.00	66.1

Table 10 Overview of reference and comparison datasets used for TS

Material	Series	Description
S355	Q_HFMI_S355_Ref	Literature data from [12]
S355	Q_HFMI_S355_Blast	actual study (HFMI-treated + blasted)
S500	Q_HFMI_S500_Ref	actual study (HFMI-treated reference series)
S500	Q_HFMI_S500_Blast	actual study (HFMI-treated + blasted)

Table 11 Statistical evaluation of fatigue tests on TS (S355 and S500) with and without blast cleaning

Series (-)	Number of tests (-)	Slope m (-)	Mean fatigue strength $\Delta\sigma_{50\%}$(MPa)	Characteristic fatigue strength $\Delta\sigma_C$(MPa)	Scatter ratio T_n(-)
Q_HFMI_S355_Ref*)	30	7.3	233.0	202.6	1:4.15
Q_HFMI_S355_Blast	14	7.4	252.5	222.1	1:2.68
Q_HFMI_S500_Ref	12	7.6	258.9	217.2	1:5.65
Q_HFMI_S500_Blast	10	7.5	265.2	228.8	1:3.85

*Data by Wendler et al. [12]

Table 12 Statistical evaluation of fatigue tests on longitudinal butt joints in HFMI-treated and AW condition made of S355 and S500

Series (-)	Number of tests (-)	Slope m (-)	Mean fatigue strength $\Delta\sigma_{50\%}$(MPa)	Characteristic fatigue strength $\Delta\sigma_C$(MPa)	Scatter ratio T_n(-)
LB_AW_S355_25	12	5.9	308.3	245.6	1:3.74
LB_HFMI_S355_25	12	6.5	301.0	242.1	1:6.06
LB_HFMI_S355_35	9	3.6	231.9/216.8 (corr.)	182.7/170.8 (corr.)	1:2.88
LB_HFMI_S500_25	5	-	-	-	-

Table 13 Statistical evaluation of fatigue tests on transverse butt joints in HFMI-treated and AW condition made of S500

Series (-)	Number of tests (-)	Slope m (-)	Mean fatigue strength $\Delta\sigma_{50\%}$(MPa)	Characteristic fatigue strength $\Delta\sigma_C$(MPa)	Scatter ratio T_n(-)
TB_AW_S500_23	9	3.7	153.1	138.2	1:1.59
TB_HFMI_S500_23	10	6.0	226.3	180.9	1:5.90
TB_HFMI_S500_35	9	5.1	244.7/227.6 (corr.)	207.3/193.8 (corr.)	1:2.55

treatment. For the investigated corrosion protection systems, the adhesion and durability in the HFMI-treated weld toe area were confirmed regardless of the treatment sequence, provided that the manufacturer's surface preparation and application requirements were met.

3 Conclusions

This study investigated the fatigue performance of HFMI-treated welded joints in offshore steel structures. The results confirm the significant improvement in fatigue strength for TB, particularly when all weld toes, including the intermediate layer, were treated. For LB welds under axial tensile loading, the AW condition already showed a high fatigue resistance, indicating a limited benefit of HFMI treatment in such cases.

Blast cleaning after HFMI treatment did not reduce the fatigue strength and was fully compatible with organic coatings and thermal-sprayed zinc, if manufacturer's specifications for surface preparation were followed.

Overall, the findings support a selective and detail-specific application of HFMI treatment in offshore steel structures.

Future work should focus on validating the combined durability of HFMI treatment and surface treatment systems under realistic offshore exposure conditions, expanding statistical evaluation to different stress ratios and joint geometries, and using numerical simulations to refine local treatment strategies for complex weld configurations.

Author contribution Daniel Löschner: fatigue testing, data analysis, writing—original draft preparation. Imke Engelhardt: supervision, project administration, funding acquisition, writing—review and editing. Diba Kopic: corrosion testing and surface analysis, writing—Chapter 1.2 and 2.1. Phillip Weidner: fatigue testing, project administration, data analysis, writing—review and editing. Stefanos Gkatzogiannis: conceptualization, experimental methodology, numerical analysis, writing—review and editing. Thomas Ummenhofer: supervision, project administration, funding acquisition. All authors read and approved the final manuscript.

Funding Open Access funding enabled and organized by Projekt DEAL. The research project "Validation of the Process Chain for the Application of High-Frequency Impact Methods in Offshore Wind Turbine Construction" was funded by the Federal Ministry of Economic Affairs and Climate Action as part of the "Industrial Collective Research" programme based on a resolution of the German Bundestag. This project IGF-Nr. 21382 N/P1454 from the Research Association for Steel Application (FOSTA), Düsseldorf, was carried out at KIT Steel and Lightweight Structures and the HM Institute of Material and Building Research. The authors are grateful to the Research Association for Steel Application (FOSTA) for their financial support as well as all the industry partners for supplying materials and performing the welding work.

Data availability The datasets generated and/or analysed during the current study are available from the corresponding author on reasonable request.

Declarations

Competing interests The authors declare that they have no competing interests.

References

1. Bourebia M, Meddah S, Mentouri Z, et al. Experimental study of the effect of shot peening parameters on the surface texture - influence on the adhesion of a paint coating. vol. 2437, 2022. https://doi.org/10.1063/5.0092375.
2. Bourebia M, Meddah S, Samia L, et al. Study of the influence of volume parameters on the paint coating adhesion, 2024, p. 61–5. https://doi.org/10.1007/978-3-031-51904-8_14.
3. Bourebia M, Meddah S, Sihem A et al (2023) Study of surface topography parameters during shot peening process and their influence on the paint coating of adhesion. Int J Adv Manuf Technol 126:3981–3993. https://doi.org/10.1007/s00170-023-11365-6
4. Ummenhofer T, Engelhardt I, Weidner P, et al. Absicherung der Prozesskette zur Anwendung höherfrequenter Hämmerverfahren bei Offshore-windenergieanlagen. FOSTA – Forschungsvereinigung Stahlanwendung e. V.; n.d.
5. DIN EN 10025–1:2005–02, Warmgewalzte Erzeugnisse aus Baustählen_- Teil_1: Allgemeine technische Lieferbedingungen; Deutsche Fassung EN_10025–1:2004 n.d. https://doi.org/10.31030/9429825.
6. DIN EN 10025–3:2019–10, Warmgewalzte Erzeugnisse aus Baustählen_- Teil_3: Technische Lieferbedingungen für normalgeglühte/normalisierend gewalzte schweißgeeignete Feinkornbaustähle; Deutsche Fassung EN_10025–3:2019 n.d. https://doi.org/10.31030/3035422.
7. Graf T, Thieme A, Schröter F (2014) Moderne Stähle für den Bau von Offshore-Konstruktionen – Herstellungsverfahren und Eigenschaften. Stahlbau 83:10–15. https://doi.org/10.1002/stab.201430003
8. Gkatzogiannis S, Weinert J, Engelhardt I et al (2019) Correlation of laboratory and real marine corrosion for the investigation of corrosion fatigue behaviour of steel components. Int J Fatigue 126:90–102. https://doi.org/10.1016/j.ijfatigue.2019.04.041

9. Weinert J. Increasing the fatigue strength of welded structural details in corrosive environments by applying high frequency mechanical impact treatment, 2021.
10. Weinert J, Gkatzogiannis S, Engelhardt I et al (2021) Investigation of corrosive influence on the fatigue behaviour of HFMI-treated and as-welded transverse non-load-carrying attachments made of mild steel S355. Int J Fatigue 151:106225. https://doi.org/10.1016/j.ijfatigue.2021.106225
11. Gkatzogiannis S, Weinert J, Engelhardt I et al (2021) Corrosion fatigue behaviour of HFMI-treated butt welds. Int J Fatigue 145:106079. https://doi.org/10.1016/j.ijfatigue.2020.106079
12. Wendler L, Löschner D, Engelhardt I et al (2023) Automatisierte Schweißnahtnachbehandlung durch höherfrequentes Hämmern. Stahlbau 92:418–426. https://doi.org/10.1002/stab.202300021
13. Hangensen PJ, Maddox SJ. IIW Recommendations on post weld fatigue life improvement of steel and aluminium structures. IIW Doc XIII-2200r7–10 2010.
14. Yildirim HC, Marquis GB (2012) Overview of fatigue data for high frequency mechanical impact treated welded joints. Weld World 56:82–96. https://doi.org/10.1007/BF03321368
15. Yildirim HC, Marquis GB (2012) Fatigue strength improvement factors for high strength steel welded joints treated by high frequency mechanical impact. Int J Fatigue 44:168–176. https://doi.org/10.1016/j.ijfatigue.2012.05.002
16. Tehrani Yekta R, Ghahremani K, Walbridge S (2013) Effect of quality control parameter variations on the fatigue performance of ultrasonic impact treated welds. Int J Fatigue 55:245–256. https://doi.org/10.1016/j.ijfatigue.2013.06.023
17. Ummenhofer T, Herion S, Hrabowski J et al (2011) REFRESH - Lebensdauerverlängerung bestehender und neuer geschweißter Stahlkonstruktionen. Verl. und Vertriebsges. mbH, Düsseldorf
18. Marquis G, Barsoum Z (2014) Fatigue strength improvement of steel structures by high-frequency mechanical impact: proposed procedures and quality assurance guidelines. Weld World 58:19–28. https://doi.org/10.1007/s40194-013-0077-8
19. Gerster P, Schäfers F, Leitner M. Pneumatic impact treatment (PIT) – application and quality assurance, 2013.
20. Schubnell J, Hanji T, Tateishi K et al (2025) Quantifying the intensity of high-frequency mechanical impact treatment. Weld World 69:125–137. https://doi.org/10.1007/s40194-024-01812-7
21. Marquis GB, Barsoum Z (2016) IIW recommendations for the HFMI treatment. Springer Singapore, Singapore. https://doi.org/10.1007/978-981-10-2504-4
22. Hobbacher AF (2016) Recommendations for fatigue design of welded joints and components. Springer International Publishing, Cham. https://doi.org/10.1007/978-3-319-23757-2
23. DASt-Richtlinien 026: Ermüdungsbemessung bei Anwendung höherfrequenter Hämmerverfahren. Stahlbau; n.d.
24. Ummenhofer T, Herion S, Weich I (2009) Schweißnahtnachbehandlung mit höherfrequenten Hämmerverfahren – Ermüdungsfestigkeit, Qualitätssicherung, Bemessung. Stahlbau 78:605–612. https://doi.org/10.1002/stab.200910074
25. DIN EN ISO 12944-2:2018-04, Beschichtungsstoffe_- Korrosionsschutz von Stahlbauten durch Beschichtungssysteme_- Teil_2: Einteilung der Umgebungsbedingungen (ISO_12944-2:2017); Deutsche Fassung EN_ISO_12944–2:2017 n.d. https://doi.org/10.31030/2718187.
26. Koerdt A, Samojluk J, An Stepec B. Future Perspectives, 2024, p. 191–232. https://doi.org/10.1201/9781003287056-16.
27. Momber A. Anforderungen an Beschichtungssysteme für Offshore-Windenergieanlagen, 2018, p. 89–99.
28. Momber A (2011) Corrosion and corrosion protection of support structures for offshore wind energy devices (OWEA). Mater Corros 62:391–404. https://doi.org/10.1002/maco.201005691
29. DIN EN ISO 8501–1:2007–12, Vorbereitung von Stahloberflächen vor dem Auftragen von Beschichtungsstoffen_- Visuelle Beurteilung der Oberflächenreinheit_- Teil_1: Rostgrade und Oberflächenvorbereitungsgrade von unbeschichteten Stahloberflächen und Stahloberflächen nach ganzflächigem Entfernen vorhandener Beschichtungen (ISO_8501–1:2007); Deutsche Fassung EN_ISO_8501–1:2007 n.d. https://doi.org/10.31030/9871577.
30. DIN EN ISO 8503–1:2013–05, Vorbereitung von Stahloberflächen vor dem Auftragen von Beschichtungsstoffen_- Rauheitskenngrößen von gestrahlten Stahloberflächen_- Teil_1: Anforderungen und Begriffe für ISO-Rauheitsvergleichsmuster zur Beurteilung gestrahlter Oberflächen (ISO_8503–1:2012); Deutsche Fassung EN_ISO_8503–1:2012 n.d. https://doi.org/10.31030/1990592.
31. DIN EN ISO 12944–5:2020–03, Beschichtungsstoffe_- Korrosionsschutz von Stahlbauten durch Beschichtungssysteme_- Teil_5: Beschichtungssysteme (ISO_12944–5:2019); Deutsche Fassung EN_ISO_12944–5:2019 n.d. https://doi.org/10.31030/3121207.
32. DIN EN ISO 12944–9:2018–06, Beschichtungsstoffe_- Korrosionsschutz von Stahlbauten durch Beschichtungssysteme_- Teil_9: Beschichtungssysteme und Leistungsprüfverfahren im Labor für Bauwerke im Offshorebereich (ISO_12944–9:2018); Deutsche Fassung EN_ISO_12944–9:2018 n.d. https://doi.org/10.31030/2778741.
33. DIN EN ISO 9227:2023–03, Korrosionsprüfungen in künstlichen Atmosphären_- Salzsprühnebelprüfungen (ISO_9227:2022); Deutsche Fassung EN_ISO_9227:2022 n.d. https://doi.org/10.31030/3402975.
34. DIN EN ISO 8503–2:2012–06, Vorbereitung von Stahloberflächen vor dem Auftragen von Beschichtungsstoffen_- Rauheitskenngrößen von gestrahlten Stahloberflächen_- Teil_2: Verfahren zur Prüfung der Rauheit von gestrahltem Stahl_- Vergleichsmusterverfahren (ISO_8503–2:2012); Deutsche Fassung EN_ISO_8503–2:2012 n.d. https://doi.org/10.31030/1857871.
35. DIN EN ISO 12944–6:2018–06, Beschichtungsstoffe_- Korrosionsschutz von Stahlbauten durch Beschichtungssysteme_- Teil_6: Laborprüfungen zur Bewertung von Beschichtungssystemen (ISO_12944–6:2018); Deutsche Fassung EN_ISO_12944–6:2018 n.d. https://doi.org/10.31030/2778740.
36. DIN EN ISO 6892–1:2020–06, Metallische Werkstoffe_- Zugversuch_- Teil_1: Prüfverfahren bei Raumtemperatur (ISO_6892–1:2019); Deutsche Fassung EN_ISO_6892–1:2019 n.d. https://doi.org/10.31030/3132591.
37. DIN EN ISO 148–1:2017–05, Metallische Werkstoffe_- Kerbschlagbiegeversuch nach Charpy_- Teil_1: Prüfverfahren (ISO_148–1:2016); Deutsche Fassung EN_ISO_148–1:2016 n.d. https://doi.org/10.31030/2482423.
38. DIN EN 10025–2:2019–10, Warmgewalzte Erzeugnisse aus Baustählen_- Teil_2: Technische Lieferbedingungen für unlegierte Baustähle; Deutsche Fassung EN_10025–2:2019 n.d.
39. DIN EN 10025–4:2023–02, Warmgewalzte Erzeugnisse aus Baustählen_- Teil_4: Technische Lieferbedingungen für thermomechanisch gewalzte schweißgeeignete Feinkornbaustähle; Deutsche Fassung EN_10025–4:2019+A1:2022 n.d.
40. DIN EN 10204:2005–01, Metallische Erzeugnisse_- Arten von Prüfbescheinigungen; Deutsche Fassung EN_10204:2004 n.d. https://doi.org/10.31030/9427568.
41. DIN EN ISO 3274:1998–04, Geometrische Produktspezifikationen (GPS)_- Oberflächenbeschaffenheit: Tastschnittverfahren_- Nenneigenschaften von Tastschnittgeräten (ISO_3274:1996); Deutsche Fassung EN_ISO_3274:1997 n.d. https://doi.org/10.31030/7433972.
42. Schubnell J, Jung M, Le CH et al (2020) Influence of the optical measurement technique and evaluation approach on the determination of local weld geometry parameters for different weld types. Weld World 64:301–316. https://doi.org/10.1007/s40194-019-00830-0
43. Weich I. Ermüdungsverhalten mechanisch nachbehandelter Schweißverbindungen in Abhängigkeit des Randschichtzustands. 2008.

44. Dürr A. Zur Ermüdungsfestigkeit von Schweißkonstruktionen aus höherfesten Baustählen bei Anwendung von UIT-Nachbehandlung 2007. https://doi.org/10.18419/OPUS-265.
45. Radaj D (1990) Design and analysis of fatigue resistant welded structures. Abington Publishing, Cambridge
46. Baumgartner J. Schwingfestigkeit von Schweißverbindungen unter Berücksichtigung von Schweißeigenspannungen und Größeneinflüssen n.d. https://doi.org/10.24406/PUBLICA-FHG-280122.
47. European Convention for Constructional Steelwork, editor. Background information on fatigue design rules: statistical evaluation. 2nd edition. Brussels: ECCS, CECM EKS; 2018.
48. DIN EN 1993–1–9:2023–03, Eurocode_3: Bemessung und Konstruktion von Stahlbauten_- Teil_1–9: Ermüdung; Deutsche und Englische Fassung prEN_1993–1–9:2023 n.d. https://doi.org/10.31030/3412135.
49. DIN EN 10225–1:2019–11, Schweißgeeignete Baustähle für feststehende Offshore-Konstruktionen_- Technische Lieferbedingungen_- Teil_1: Bleche; Deutsche Fassung EN_10225–1:2019 n.d. https://doi.org/10.31030/3003767.